

Mechanical Performance of Styrene-2-Ethylhexyl Acrylate Polymers Synthesized by Semicontinuous Emulsion Polymerization Varying Feed Composition

**Carlos F. Jasso-Gastinel, Ignacio Reyes-González, and
Luz C. López-Ureta**

Chemical Engineering Department, Universidad de Guadalajara,
Guadalajara, México

Luis J. González-Ortiz

Chemistry Department, Universidad de Guadalajara, Guadalajara, México

Octavio Manero-Brito

Materials Research Institute, Universidad Nacional Autónoma de México,
México D. F., México

Abstract: A semicontinuous emulsion process varying comonomer feed composition in the course of the reaction is used here to produce copolymer chains of different composition as conversion proceeds. Polymeric material global composition and evidence of branching are determined by $^1\text{H-NMR}$. The \overline{M}_n determined by GPC is beyond the range where the mechanical properties depend on molecular weight. Static and dynamic mechanical properties of variable composition copolymers exhibit highly improved copolymer type behavior for all tested

Received 11 January 2006; accepted 14 May 2006.

This work has been supported by Conacyt and the University of Guadalajara under projects 32772-U and PROPESTI 2004. The authors thank Carmen Vázquez-Ramos for running dynamic tests.

Address correspondence to Carlos F. Jasso-Gastinel, Chemical Engineering Department, Universidad de Guadalajara, Blvd. Gral. Marcelino García Barragán # 1451, Guadalajara, Jalisco C. P. 44430, México. E-mail: carlos.jasso@cucei.udg.mx

compositions (styrene content between 30 and 85 wt%), showing high superiority of the mechanical performance in comparison with random copolymers and two-stage polymers of equivalent composition, synthesized also by emulsion polymerization.

Keywords: Copolymerization; Core-shell polymers; Emulsion polymerization; Mechanical properties; NMR; P2EHA

INTRODUCTION

The synthesis of engineering materials combining the properties of two components has different directions.^[1,2] Different types of polymerizations and numbers of stages have been used to obtain polymeric materials.^[3-5] If a variation in composition is pursued throughout the bulk of a polymer, an additional parameter of study would have to be considered.^[6]

To improve the properties offered by random copolymers (RC), block and graft copolymers were developed in the 1960s, expanding potential polymer applications.^[1] Later on, polymer blends of homogeneous composition were obtained by sequential bulk polymerization, offering a method that could be used for any pair of monomers, to obtain better mechanical properties than those of equivalent RC.^[7] However, achieving a gradient composition throughout the bulk polymer, an additional mechanical improvement was obtained.^[7,8] Such outstanding behavior may be obtained by maintaining phase separation at the microscopic level, thus increasing the interaction between the components.^[9] In gradient composition systems, the homopolymer contribution can be optimized by designing the gradient in a specific way.^[10-12] In bulk polymerization, one way to reach a desired composition gradient is by controlling the diffusion of a second monomer in a host polymer, followed by an in situ reaction.^[13] Pursuing mechanical modification, the second monomer diffusion approach has been used in both amorphous^[7,8,10,11,13] and crystalline polymers.^[14] During polymer processing, the gradients in morphology have been formed by annealing molded sheets^[15] or by slow crystallization in injection molding.^[16]

In suspension polymerization, the gradient composition concept has been applied in the preparation of small beads to release in a controlled way a pharmaceutical drug.^[17] In a similar manner, studies at particle level, carried out in emulsion polymerization, have shown the potential of using seed latexes to prepare two component materials in two-stage processes, pursuing property combination. In seeded emulsion polymerizations (SEPs), two-phase particles are commonly obtained as a consequence of polymer incompatibility. Unfortunately, different particle

morphologies and, consequently, different system properties may be obtained at the end of the reaction due to the many variables involved in such polymerization processes.^[18–20] Changes in the monomer/seed ratio, type and amount of emulsifier, and feed mode of emulsion components are just some of the different process parameters controlling the development of particle morphology throughout SEP,^[18–21] which is, in fact, the result of the balance between several kinetic and thermodynamic factors.^[22–24] In addition, for a given chemical system, the mechanical behavior of the polymer bulk obtained through a two-component SEP depends, among other factors,^[24–29] on the morphology of particles used to prepare such bulk.

Some semicontinuous seeded emulsion copolymerizations have been focused on the production of copolymers with constant composition.^[30–32] However, based on the favorable mechanical behavior shown by systems of variable composition synthesized through sequential bulk polymerizations,^[7,8,10,11] it can be expected that a synergistic effect could also be obtained when a copolymer is synthesized by seeded emulsion copolymerization, provided that the particles contain copolymer chains of a wide range of compositions. One way to favor that scheme is to use a semicontinuous process promoting in the polymerization locus (e.g., polymer particle) composition changes throughout the reaction.

The 2-ethylhexyl acrylate (2EHA) is a monomer that promotes high elasticity in copolymer chains that include mers exhibiting high energy rotation barriers (e.g., methyl methacrylate or styrene); this characteristic has been recently utilized in adhesives.^[33,34] The application of that idea to high molecular weight polymers would allow the synthesis of polymers containing 2EHA mers in order to prepare tough plastics or reinforced rubbers.

In this work, the polymerization of styrene-2EHA is studied. A procedure that involves a semicontinuous monomer feed is proposed to obtain copolymer chains of different compositions. Global composition and evidence of branched polymer formation are determined by ¹H-NMR (nuclear magnetic resonance). Mechanical and rheological properties are measured and compared with those of equivalent RC materials (prepared by batch emulsion copolymerization) and of polymers prepared by two-stage SEPs (T-S).

EXPERIMENTAL SECTION

Materials

Styrene (from Pemex) and 2-ethylhexyl acrylate acquired from BASF (for both, purity >99.5%) were treated with ion-exchange resin (from

Aldrich) to remove inhibitor. Polyoxyethylene-20-sorbitan monolaurate (Tween-20) from ICI de México was used as emulsifier. Depending on the polymerization recipe, potassium persulfate initiator or potassium persulfate and sodium bisulfite redox initiation system were used; both chemical compounds were acquired from Aldrich.

Preparation

The T-S latexes were prepared at 60°C in a 10 L steel reactor. For that purpose, the required amount of polystyrene (PS) seed particles was synthesized by batch emulsion polymerization, using Tween-20 as emulsifier and potassium persulfate (KPS) as initiator; details of recipes are shown in Table I. After each seed was synthesized, the required amount of the second monomer was added to the reactor while stirring; 2EHA addition (second monomer) was carried out over one hour, maintaining an almost constant feed flow. After 2EHA addition was finished, an extra swelling period of two hours was applied before the addition of the redox initiation system and of the required amount of sodium bicarbonate (second stage polymerization recipe is shown in Table I); this addition indicated the start of the second stage polymerization, which continued until the conversion was >97%.

Variable composition copolymers (VCC) were also prepared at 60°C using a multistep procedure by varying feed composition in each step. First, polystyrene seed latexes were prepared at 60°C by batch emulsion polymerization, using the recipe shown in Table I. The required amount of polystyrene seed latex and an aqueous solution containing 25 g of NaHCO₃ were charged to the reactor (the polymer contained in the latex represented 20 wt% of the final polystyrene content). Then, comonomers were simultaneously added to reactor, using two Masterflex L/S peristaltic pumps in a semicontinuous process. To obtain copolymer chains with a certain composition pattern, feed composition was changed in a step way, as shown in Figure 1, varying the amount of each monomer fed on every step, following a linear pattern (increasing for 2EHA and decreasing for styrene). At the start of each step, the following liquids were sequentially added to reactor: (a) 9.1 g of Tween-20 (to prevent coagulation), (b) 15 mL of an aqueous solution of potassium persulfate (containing 2.7 g of salt), and (c) 15 mL of an aqueous solution of sodium bisulfite (containing 1.28 g salt). Polymerization recipes used to prepare VCC materials are shown in Table I.

RC materials were synthesized in a 10 L reactor using a batch emulsion copolymerization. Reaction recipes are also shown in Table I. For these reactions, the required amounts of surfactant (Tween-20), NaHCO₃, and water were added to the reactor (with temperature

Table I. Polymerization recipes used in this work

Substance	Load added (g)			
	T-S latexes			
Styrene/2-ethylhexyl acrylate ratio	85/15	70/30	50/50	30/70
PS seed latex used to synthesize T-S latexes				
Material code	T-S85	T-S70	T-S50	T-S30
Styrene (S)	1360	1120	800	480
Tween-20	44.9	37.0	26.4	15.8
Potassium persulfate (KPS)	13.6	11.2	8.0	4.8
NaHCO ₃	10.2	8.4	6.0	3.6
Water	5850	5850	5850	5850
Second-stage polymerization				
2-Ethylhexyl acrylate (2-EHA)	240	480	800	1120
KPS	1.80	3.40	5.8	8.2
Sodium bisulfite	0.80	1.60	2.8	4.0
NaHCO ₃	1.5	2.8	4.8	6.8
VCC latexes				
PS seed latex used to synthesize VCC latexes				
S	1125			
Tween-20	37.1			
KPS	11.25			
NaHCO ₃	8.4			
Water	6675			
Material code	VCC85	VCC70	VCC50	VCC30
PS in seed latex	510	420	300	180
S	2040	1680	1200	720
2-EHA	450	900	1500	2100
Tween-20	100	100	100	100
KPS	29.7	29.7	29.7	29.7
Sodium bisulfite	14.1	14.1	14.1	14.1
NaHCO ₃	25	25	25	25
Water (total)	4000	4000	4000	4000
RC latexes				
Material code	RC 85	RC 70	RC 50	RC 30
S	2550	2100	1500	450
2-EHA	450	900	1500	2550
Tween-20	100	100	100	100
KPS	30	30	30	30
NaHCO ₃	25	25	25	25
Water (total)	4000	4000	4000	4000

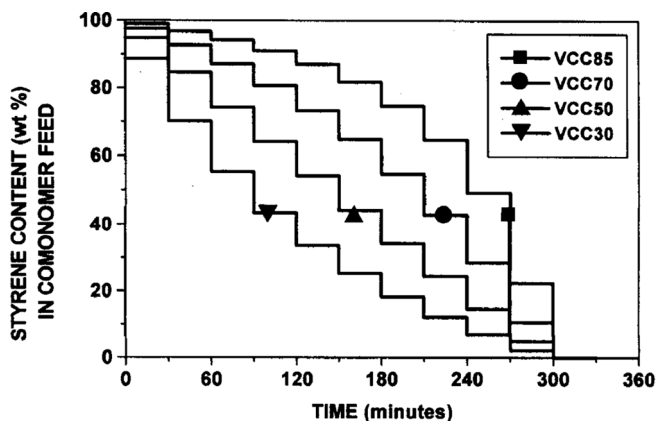


Figure 1. Instantaneous feed composition as a function of reaction time, for styrene-2-ethylhexyl acrylate VCC synthesis. For materials code see Table I.

controlled at 60°C). Afterwards, such components were stirred for one hour before the comonomer mixture was added; this addition was carried out over 30 minutes. Then, to start the reaction, an aqueous solution (100 mL) containing the required amount of potassium persulfate was added to the system.

Characterization

Global composition of synthesized polymers was obtained by $^1\text{H-NMR}$ (Varian Gemini 2000). Number-average molecular weight of final polymeric materials was measured by gel permeation chromatography (Perkin Elmer Series 410, equipped with an LC-30 refractive index detector and coupled with a light scattering unit from Wyatt Technologies). For mechanical tests of the coagulated polymeric materials, polymer plates were prepared by compression molding (Schwabenthan polystat 200 T), using a $20 \times 20 \times 0.3 \text{ cm}^3$ mold. Stress-strain tests were carried out on a universal testing machine (United FM), following ASTM D638, using a 0.083 cm/s cross-head speed. Mechanodynamic measurements with a Dynamomechanical Analyzer (DMA, TA model Q800) were carried out using the three-point bending deformation mode at 1 Hz. Storage (G') and loss (G'') moduli were measured as a function of temperature.

RESULTS AND DISCUSSION

For each reaction, global composition was determined by $^1\text{H-NMR}$. For styrene mer quantification, the broad signal area between 6.1 and

7.2 ppm was calculated (aromatic hydrogens), while the methyl triplet signal (from two methyl groups) appearing at approximately 0.9 ppm was used to evaluate the 2EHA mer. It was found that the global compositions are in agreement with the amount of comonomers added to the reactor. In Figure 2, $^1\text{H-NMR}$ spectra of PS, poly(2-ethylhexyl acrylate) (P2EHA; polymerized in bulk at 60°C) and final samples of representative T-S, RC, and VCC reactions can be seen. Normalized areas of characteristic peaks of spectra shown in Figure 2 are included in Table II.

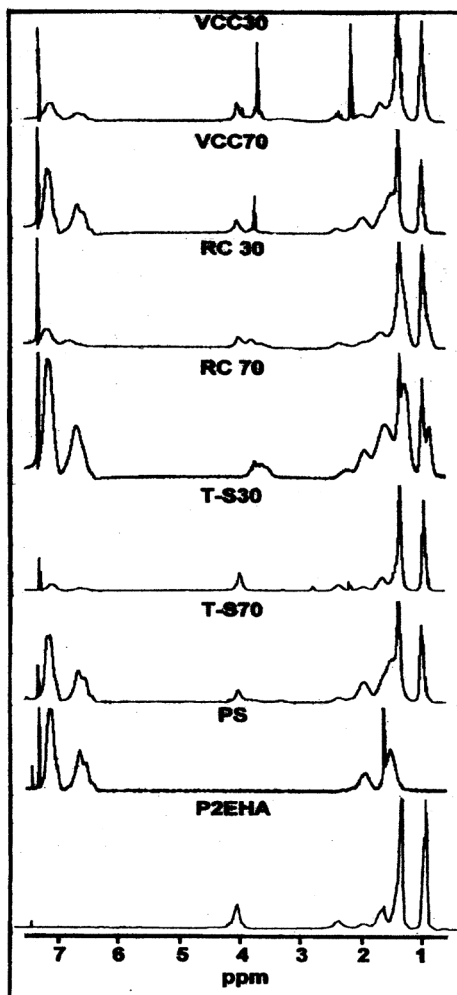


Figure 2. $^1\text{H-NMR}$ spectra of P2EHA, PS, and final samples of the T-S70, T-S30, RC 70, RC 30, VCC70, and VCC30 reactions. For materials code see Table I.

Table II. Normalized areas of $-\text{C}_6\text{H}_5$, $-\text{OCH}_2-$, and $-\text{CH}_3$ signals for spectra shown in Figure 2

Material code	$-\text{C}_6\text{H}_5$ (6.2–7.2 ppm)	$-\text{OCH}_2$ (4.0 ppm)	$-\text{CH}_3$ (0.9–1.0 ppm)
RC 30	29	9	62
RC 70	75	0	25
VCC30	39	12	49
VCC70	72	5	23
T-S30	22	19	59
T-S70	73	6	21

For spectra of VCC and RC materials included in Figure 2, the ratio between the signal area at 4 ppm (assigned to $-\text{OCH}_2-$ chemical groups of 2EHA) and the one appearing at approximately 0.9 ppm (due to two methyl groups of 2EHA) is considerably lower than the theoretical ratio (2/6) that would be expected if only linear polymer chains had been formed during the reactions (see Table II); in fact, in the RC 30 sample, the peak at 4.0 ppm cannot be found in its spectrum. Moreover, for two-component material spectra, the presence of “new” peaks can be clearly observed (between approximately 3.2 and 3.8 ppm); that situation can only be explained if one or more side reactions occur during the polymerization (e.g., those forming branched polymer). Branched polymer formation has been reported during homo^[35] and copolymerizations of 2EHA.^[34] However, in spectra for T-S materials, the ratios between the areas of signals appearing at 4.0 and 0.9 ppm are close to the theoretical ratio, showing that the reactions of $-\text{OCH}_2$ chemical groups of 2EHA mer can be neglected.

As the relation between molecular weight and mechanical properties of polymers is a complex function up to a critical value of molecular weight, above which maximum property values are obtained,^[26] the number-average molecular weights of synthesized polymers are shown in Table III. These values clearly exceed the critical number-average degree of polymerization that is required to form enough entanglements and assure that mechanical properties are not affected by molecular size.^[25] For this reason, polymer molecular weight is not a factor influencing the mechanical properties measured in this work. Therefore, the differences in mechanical behavior are mainly a consequence of the structural change obtained due to the type of synthesis used.

In Figures 3 and 4, stress-strain properties of homopolymers and RC, T-S, and VCC synthesized materials can be compared. All two-component material curves allocate between those of the homopolymers; RC samples present the weakest mechanical behavior among the two-component materials (comparing equivalent compositions), while the VCC materials consistently present the strongest and toughest behavior.

Table III. Number-average molecular weight (\overline{M}_n) for two-component polymers

Material code	VCC85	VCC70	VCC50	VCC30
$M_n \times 10^{-5}$ (g/mol)	4.0	3.0	3.2	4.7
Material code	T-S85	T-S70	T-S50	T-S30
$M_n \times 10^{-5}$ (g/mol)	1.8	2.1	1.8	1.8
Material code	RC 85	RC 70	RC 50	RC 30
$M_n \times 10^{-5}$ (g/mol)	3.4	4.6	5.1	4.3

In Figure 3, VCC30 (Figure 3(a)) and VCC50 (Figure 3(b)) material curves present, respectively, the highest initial slope, with similar elongation capacity to the equivalent T-S polymers. The RC materials exhibit the lowest slopes and the highest ultimate strain.

All materials with 30 wt% of styrene show an elongation capacity beyond 300% (Figure 3(a)), and with 50 wt% of styrene they maintain a considerable elongation capacity (>200%; Figure 3(b)), while offering a high increase in modulus and ultimate stress (especially VCC material).

A further increase in modulus for all two-component materials can be observed for compositions with 70 wt% of styrene (Figure 4(a)), but presenting a marked decrease in the elongation capacity. The RC material presents the lowest elongation along with the lowest modulus. Again, the VCC70 curve is substantially above the curves of the other two-component materials, denoting the advantage of the VCC synthesis approach. The highest Young's modulus value for the two component polymers is obtained with materials containing 85 wt% of styrene (Figure 4(b)). For this composition, the T-S85 curve is closer to the RC curve than to the VCC curve. This shows that even for materials with a small amount of rubbery component, the VCC synthesis approach is better than the T-S approach. Furthermore, compared to PS, the T-S85 polymer loses 74% in modulus, while the VCC85 material loses only 45%, although they present similar elongation capacity.

The comparison of modulus, ultimate stress, ultimate strain, and area under the stress-strain curves (toughness) is shown in Table 4. It is clear that RC materials offer an intermediate response between the pure polymers and T-S materials present an improved performance with respect to equivalent RC samples. However, VCC materials present outstanding values, showing superiority over the other two-component materials in modulus, ultimate stress, and toughness, maintaining rupture strains similar to T-S materials. The toughness values of VCC materials are clearly above those of equivalent T-S materials (62% for VCC30/T-S30 and 114% for VCC50/T-S50), although for high styrene content materials, its superiority is not so high (44% for VCC70/T-S70 and 22% for VCC85/T-S85). Such results are a consequence of the very

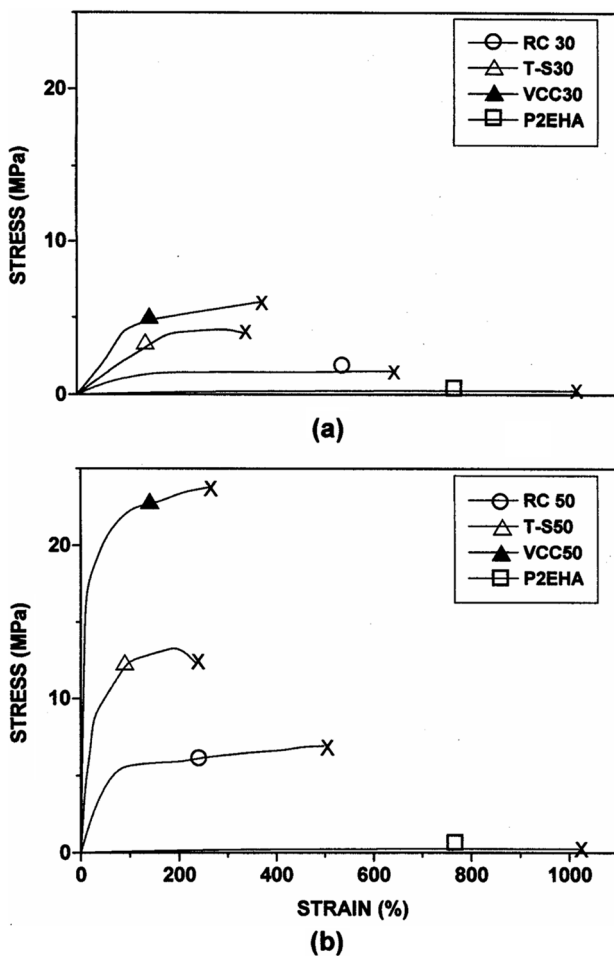
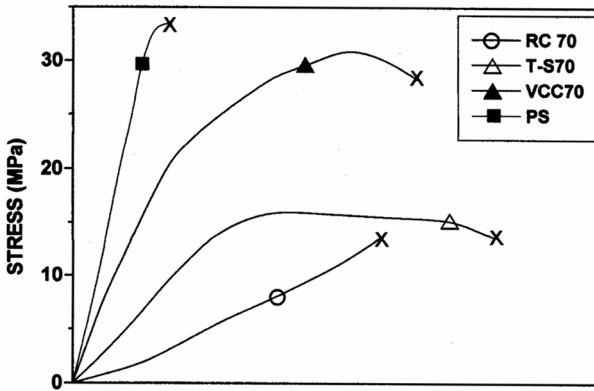
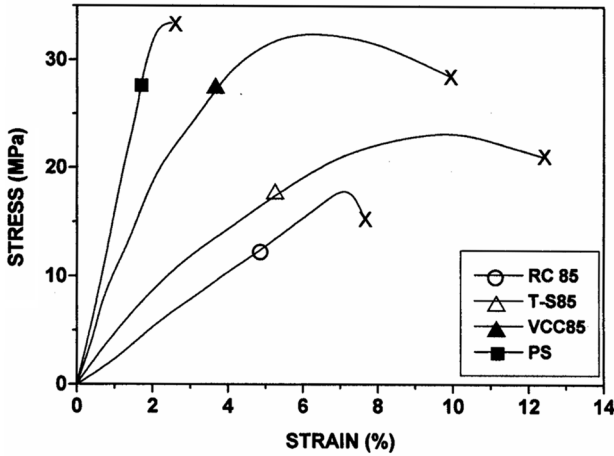


Figure 3. Stress-strain behavior for (a) P2EHA and two-component polymers containing 30 wt % of styrene and (b) P2EHA and two-component polymers containing 50 wt% of styrene. For materials code see Table I.

high modulus along with a considerable elongation capacity (presented by the VCC materials). These toughness results are very special because VCC materials do not present the highest rupture strain for any of the studied compositions. It is also important to notice, for all types of synthesis, the dramatic behavior change of the materials containing more than 50 wt% of styrene. High rupture strain and toughness values are obtained for materials containing 30 and 50 wt% of styrene, and very low values of such parameters (between one and two orders of magnitude lower) are obtained for materials containing 70 and 85 wt% of styrene.



(a)



(b)

Figure 4. Stress-strain behavior for (a) PS and two-component polymers containing 70 wt% of styrene and (b) PS and two-component polymers containing 85 wt% of styrene. For materials code see Table I.

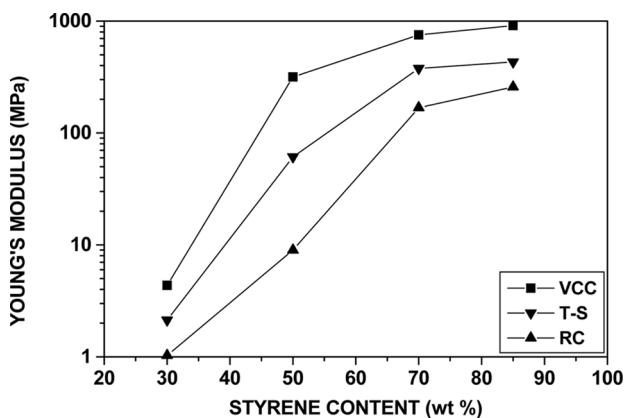
Figure 5 shows Young's modulus behavior as a function of composition for RC, T-S, and VCC materials. Using a semilogarithmic plot, all differences in modulus can clearly be seen. Superiority of VCC materials' performance is consistent for the whole composition spectrum, whereas T-S materials present intermediate values between VCC and RC materials. Moreover, when changing from 30 to 50 wt% of styrene, the VCC curve presents the highest increment in modulus (2.5 times higher than the one corresponding to the T-S material), which could be associated with the type of copolymer chain structure. Such synergistic effect does

Table IV. Young's modulus, ultimate stress, ultimate strain, and toughness of RC, T-S, and VCC materials; for codes see Table I

Material code	Young's modulus (MPa)	Ultimate stress (MPa)	Ultimate strain (%)	Toughness $\times 10^{-6}$ (J/m ³)
PS	1.6×10^3	34	2.5	0.49
P2EHA	7.7×10^{-2}	2.4×10^{-1}	1.0×10^3	2.0
RC 30	1.0	1.5	6.5×10^2	8.6
T-S30	2.1	4.0	3.4×10^2	10
VCC30	4.4	6.0	3.7×10^2	16
RC 50	9.0	6.9	5.0×10^2	29
T-S50	61	12	2.4×10^2	27
VCC50	3.2×10^2	24	2.6×10^2	57
RC 70	1.7×10^2	14	8.2	0.5
T-S70	3.8×10^2	14	11	1.5
VCC70	7.5×10^2	28	9.2	2.1
RC 85	2.6×10^2	15	7.7	0.74
T-S85	4.3×10^2	21	12	2.1
VCC85	9.1×10^2	28	10	2.5

not appear in the whole composition range for the other two-component materials. The mechanostatic properties enhancement obtained for variable composition polymers agrees with the results obtained for other systems prepared by bulk polymerization.^[7,8,10,11]

Rheological behavior of synthesized materials can be seen in Figures 6–9. Storage modulus as a function of temperature is presented in Figures 6 and 7 for homopolymers and RC, T-S, and VCC synthesized materials. In Figure 6, performance comparison for materials with

**Figure 5.** Young's modulus as a function of styrene content for the three types of synthesized materials. For materials code see Table I.

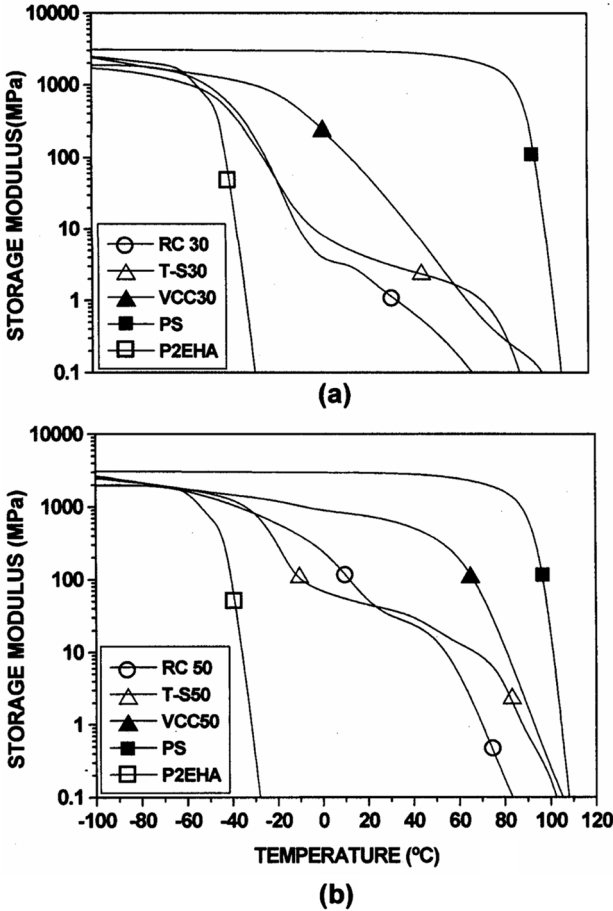


Figure 6. Storage modulus for (a) PS, P2EHA, and two-component polymers containing 30 wt% of styrene and (b) PS, P2EHA, and two-component polymers containing 50 wt% of styrene. For materials code see Table I.

30 wt% of styrene shows that two-component materials behave closer to the P2EHA curve than to the PS curve (Figure 6(a)). Nevertheless, RC and T-S polymers follow similar trajectories up to 20°C. Then, the T-S material exhibits a long plateau, until its modulus presents another fall in the vicinity of 80°C. However, the RC material shows a steady decrement beginning at 20°C. Nonetheless, the VCC30 curve shows a high modulus value beyond that of the other two-component materials (in the low temperature region) before its value presents a steady decrease, to finally cross the T-S30 curve at 65°C. For this reason, G' of the VCC30 material is clearly above the G' of the T-S30 polymer, between -40° and 60°C.

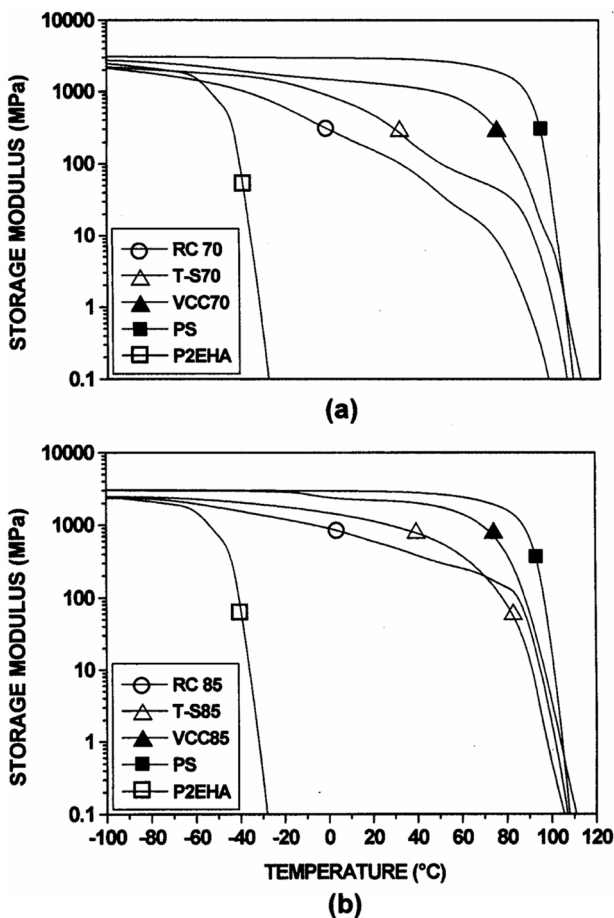


Figure 7. Storage modulus for (a) PS, P2EHA, and two-component polymers containing 70 wt% of styrene and (b) PS, P2EHA, and two-component polymers containing 85 wt% of styrene. For materials code see Table I.

For 50 wt% of styrene materials (Figure 6(b)), RC and T-S polymers behave similarly, although the T-S50 polymer shows a long plateau between -10° and 80°C . Again, the VCC curve shows high modulus beyond that of the other two component polymers, and for this composition, it shows a high value up to 50°C . In addition, the VCC curve is above the other ones for the whole temperature range. Moreover, the VCC curve is much closer to the PS curve than to the P2EHA curve, denoting a synergistic behavior. It is also important to mention that, for the 15° – 65°C temperature range, G' values of the VCC50 material are more than 10 times the G' values of the other two-component materials. The synergistic effect can also be noticed

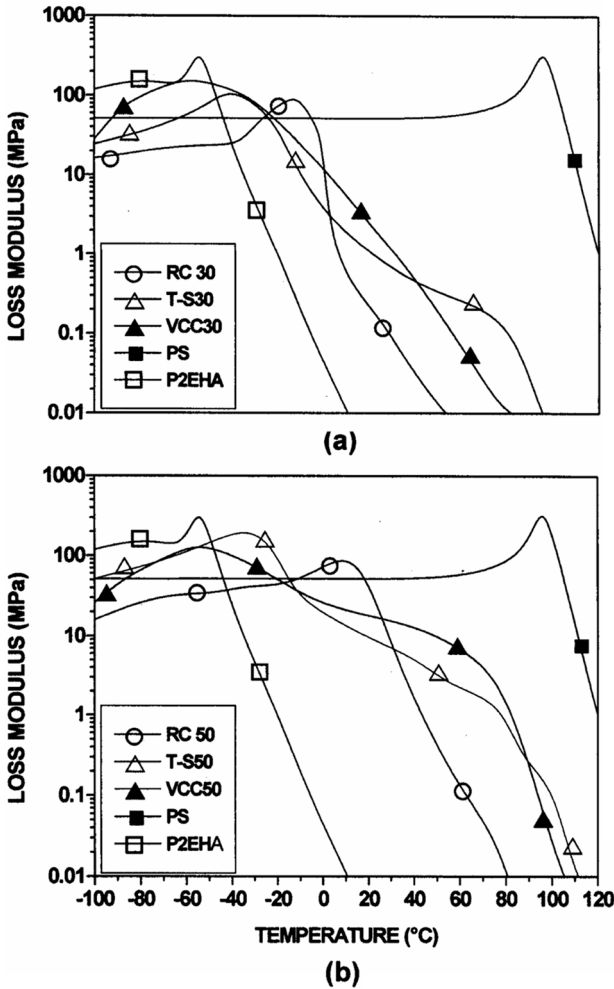


Figure 8. Loss modulus for (a) PS, P2EHA, and two-component polymers containing 30 wt% of styrene and (b) PS, P2EHA, and two-component polymers containing 50 wt% of styrene. For materials code see Table I.

in Figure 6(a), because the curve for VCC30 material is almost in the middle of P2EHA and PS curves, although it only contains 30wt% of styrene. In VCC materials, component interaction is improved by the presence of copolymer chains within a wide range of compositions (wider than in RC materials), which is different than the case where two homopolymers interact at their interphase (e.g., T-S polymers).

In Figure 7, as a consequence of the high styrene global percentage, curves for all two-components materials appear near to the PS curve. The

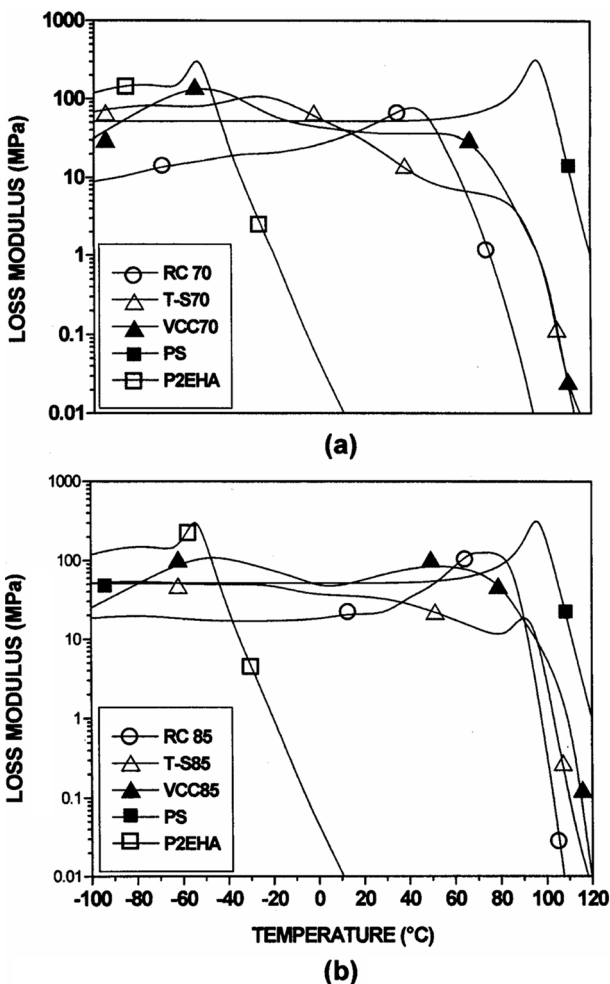


Figure 9. Loss modulus for (a) PS, P2EHA, and two-component polymers containing 70 wt% of styrene and (b) PS, P2EHA, and two-component polymers containing 85 wt% of styrene. For materials code see Table I.

tendency to form a second plateau decreases in materials with 70 wt% of styrene (Figure 7(a)) and almost disappears in materials with 85 wt% of styrene (Figure 7(b)). In Figure 7(a), VCC70 material shows a marked superiority over the other two-component polymers, from 10° to 80°C, which is a temperature range for many polymer applications. The VCC material superiority can also be noticed in samples with 85wt% of styrene. Below 0°C, the curve for VCC85 material is quite similar to the PS line and is close to it up to 50°C. However, the modulus decrease

for T-S and RC materials starts around -10°C , with the T-S polymer curve above the curve of the RC material.

Examining storage modulus values in a sequential mode from plot 6(a) to 7(b), it can be observed that, as styrene content increases, the G' curve for each of the two-component materials moves from the vicinity of the P2EHA curve to the vicinity of the PS curve. In addition, for the whole temperature range, the difference between the PS G' value and the G' value of the respective two-component material (RC, T-S, or VCC) is smaller as styrene content increases.

For RC materials (in which the instantaneous composition is mainly influenced by monomer relative reactivities), the incipient second plateau appears at higher temperature values as styrene content increases (although such a plateau does not appear at 85 wt% of styrene content). In addition, the G' value of the second plateau increases with styrene content. The same pattern is followed by T-S materials, although the second plateau is longer in every case, denoting a clearly defined two-phase material behavior. However, G' curves determined for all VCC materials show only one plateau, which can be explained in terms of copolymer chain formations covering a very wide range of compositions. Nevertheless, VCC materials show higher G' values than RC and T-S materials.

In Figures 8 and 9, loss moduli of homopolymers, RC, TS, and VCC synthesized materials are shown as a function of temperature. Homopolymers show their corresponding glass transition temperature (T_g) at the maximum energy dissipation value (^[36]; “peak” value), while the two-component polymeric materials show different behavior depending on their synthesis method and global composition. Random copolymers in all cases show only one maximum energy dissipation value, which appears at a temperature that increases as styrene content increases. For T-S polymers, two wide peaks appeared in the vicinity of the peaks that correspond to the homopolymers T_g (above P2EHA T_g and below PS T_g). In Figure 8(a), the VCC30 curve shows a wide peak in the low temperature region, denoting copolymer formation (its peak is even wider than the one corresponding to the RC30 sample), and, consequently, the G'' decrease is gradual (less steep than the one corresponding to the T-S30 polymer). In addition, the T-S30 curve shows a second “peak” at approximately 80°C . In Figure 8(b), the behavior of two-component polymers is similar to that in Figure 8(a), although for the T-S50 polymer, the peak appearing at the high temperature region is almost imperceptible. Once again, the equivalent VCC material shows a gradual decrease in modulus after the first “peak,” showing a high G'' value up to 75°C .

Figure 9(a) shows that the high styrene content of T-S70 polymer allows the maintenance of a considerable G'' value up to 85°C whereas the curve for VCC70 material shows a horizontal trajectory (above the T-S70 curve beginning at 20°C), after a wide peak at low temperature

(-50°C), continuing in that way up to 70°C . Then, its G'' value decreases, “matching” the T-S70 curve at 87°C . Because of the very high styrene content in the two-component materials of Figure 9(b), high G'' values at temperatures as high as 75°C are obtained. The VCC85 material shows the highest dissipation capacity up to 60°C (denoting the styrene influence). For the T-S85 polymer, there is a very weak G'' variation in the low temperature region, showing a clear peak at 90°C (close to PS T_g).

It can be seen for the three types of materials that the effect of styrene content in loss modulus behavior is similar to the effect observed for storage modulus; the maintenance of high G'' values shows a direct relationship with styrene content.

The static and dynamic mechanical properties panorama for VCC materials synthesized with the approach used in this work indicates that the performance increase (with respect to T-S and RC materials) is remarkable. Such effect is possible because styrene-rich copolymer chains contribute to increase material rigidity (that is, Young's and storage moduli increase beyond those of the T-S and RC materials), while copolymer chains rich in 2 EHA contribute to obtaining high deformation capacity. Polymer particles with a continuous composition change pattern in the course of the reaction were obtained (VCC), giving as a result an improvement of the mechanical performance of two-component polymers.

CONCLUSIONS

A semicontinuous emulsion polymerization process varying feed composition is feasible for the preparation of “tailor-made copolymers.” By applying an adequate composition variation pattern, a synergistic effect was reached in mechanical properties of variable composition copolymers. This behavior of the VCC materials can be explained in terms of the favorable contribution of significant amounts of chains rich in one of the respective components changing composition in a gradual manner, containing in the final polymer both types of chains rich in one component. For all ranges of composition, VCC materials showed a clear mechanical superiority over RC and T-S materials.

REFERENCES

- [1] Ceresa, R. J. and W. R. Grace. (1973). In *Block and Graft Copolymerization*, eds. R. J. Ceresa, Vol. 2, pp. 485–528. New York: Wiley Interscience.
- [2] Sperling, L. H. (1994). In *Interpenetrating Polymer Networks*, ed. D. Klemperer, L. H. Sperling, and L. A. Utracki. pp. 3–77. Washington, D.C.: American Chemical Society.

- [3] Schildknecht, C. E. (1977). *Polymerization Processes*, eds. C. E. Schildknecht, and I. Skeist. New York: Wiley-Interscience.
- [4] Sundberg, D. C. and Y. G. Durant. (2003). Latex particle morphology, fundamental aspects: A review. *Polym. React. Eng.* **11**, 379–432.
- [5] Odian, G. (2004). *Principles of Polymerization*, 4th ed. Hoboken, N.J.: Wiley-Interscience, pp. 1–38.
- [6] Shen, M. and M. B. Bever. (1972). Gradient polymers. *J. Mater. Sci.* **7**, 741–746.
- [7] Akovali, G., K. Biliyar, and M. Shen. (1976). Gradient polymers by diffusion polymerization. *J. Appl. Polym. Sci.* **20**, 2419–2427.
- [8] Jasso, C. F., D. Hong, and M. Shen. (1979). In *Multiphase polymers*, pp. 443–453. Washington D.C.: American Chemical Society.
- [9] Manson, J. A. and L. H. Sperling. (1976). *Polymer Blends and Composites*, New York: Plenum Press. pp. 237–270.
- [10] Martin, G. C., E. Enssani, and M. Shen. (1981). Mechanical behavior of gradient polymers. *J. Appl. Polym. Sci.* **26**, 1465–1473.
- [11] Jasso, C. F., J. J. Martínez, E. Mendizábal, and O. Laguna. (1995). Mechanical and rheological properties of styrene/acrylic gradient polymers. *J. Appl. Polym. Sci.* **58**, 2207–2212.
- [12] Jasso-Gastinel, C. F. (1996). In *Polymeric Materials Encyclopedia*, ed. J. C. Salamone, Vol. 4, pp. 2849–2856. Boca Raton: CRC Press.
- [13] Jasso, C. F., J. Valdéz, J. H. Pérez, and O. Laguna. (2001). Analysis of butyl acrylate diffusion in a glassy polystyrene matrix to predict gradient structure. *J. Appl. Polym. Sci.* **80**, 1343–1348.
- [14] Pluta, M., P. Milczarek, and M. Kryszewski. (1987). Polyethylene-polystyrene gradient polymers. III: Mechanical and rheo-optical studies of relaxation processes. *Colloid. Polym. Sci.* **265**, 490–497.
- [15] Xie, X.-M., M. Matsuoka, and K. Takemura. (1992). Formation of gradient phase structure during annealing of a polymer blend. *Polymer* **33**, 1996–1998.
- [16] Ulcer, Y., J. Miao, M. Cakmak, and C. M. Hsiung. (1996). Structural gradients developed in injection-molded syndiotactic polystyrene (sPS). *J. Appl. Polym. Sci.* **60**, 669–691.
- [17] Mueller, K. F. and S. J. Heiber. (1982). Gradient-IPN-modified beads: Their synthesis by diffusion-polycondensation and function as controlled drug delivery agents. *J. Appl. Polym. Sci.* **27**, 4043–4064.
- [18] Kamei, S., M. Okubo, and T. Matsumoto. (1986). Production of anomalous particles in the process of emulsifier-free emulsion copolymerization of styrene and 2-hydroxyethyl methacrylate. *J. Polym. Sci. Part A Polym. Chem. Ed* **24**, 3109–3116.
- [19] Cho, I. and K.-W. Lee. (1985). Morphology of latex particles formed by poly(methyl methacrylate) - seeded emulsion polymerization of styrene. *J. Appl. Polym. Sci.* **30**, 1903–1926.
- [20] Chen, Y. C., V. Dimonie, and M. S. El-Aasser. (1992). Role of surfactant in composite latex particle morphology. *J. Appl. Polym. Sci.* **45**, 487–499.
- [21] Jönsson, J.-E., H. Hassander, and B. Törnell. (1994). Polymerization conditions and the development of a core-shell morphology in PMMA/PS latex particles. 1: Influence of initiator properties and mode monomer addition. *Macromolecules* **27**, 1932–1937.

- [22] Chen, Y. C., V. Dimonie, and M. S. El-Aasser. (1993). Development of morphology in latex particles: The interplay between thermodynamic and kinetic parameters. *Polym. Int.* **30**, 185–194.
- [23] Dimonie, V. L., E. S. Daniels, O. L. Shaffer, and M. S. El-Aasser. (1997). In *Emulsion Polymerization and Emulsion Polymers*, eds. P. A. Lovell, and M. S. El-Aasser. pp. 293–323. New York: John Wiley.
- [24] González-Ortiz, L. J., and J. M. Asua. (1996). Development of particle morphology in emulsion polymerization. III: Cluster nucleation and dynamics in polymerizing systems. *Macromolecules* **29**, 4520–4527.
- [25] Nielsen, L. E. and R. F. Landel. (1994). *Mechanical Properties of Polymers and Composites*, 2nd ed. New York: Marcel Dekker Inc. pp. 44–49.
- [26] Martin, J. R., J. F. Johnson, and A. R. Cooper. (1972). *J. Macromol. Sci. Rev. Macromol. Chem.* **C8**, 57–199.
- [27] Day, R. J., P. A. Lovell, and D. Pierre. (1997). Toughening of epoxy resins using particles prepared by emulsion polymerization: Effects of particle surface functionality, size and morphology on impact fracture properties. *Polym. Inter.* **44**, 288–299.
- [28] González-León, J. A., S. W. Ryu, S. A. Hewlett, S. H. Ibrahim, and A. M. Mayes. (2005). Core shell polymer nanoparticles for baroplastic processing. *Macromolecules* **38**, 8036–8044.
- [29] Min, T. I., A. Klein, M. S. El-Aasser, and J. W. Vanderhoff. (1983). Morphology and grafting in (poly (butyl acrylate)-polystyrene) core/shell emulsion polymerization. *J. Polym. Sci. Part A, Polym. Chem. Ed.* **21**, 2845–2861.
- [30] Galimberti, F., M. Morbidelli, A. Siani, and G. Storti. (1998). Applications of composition control to the styrene-butyl acrylate emulsion copolymerization. *Chem. Eng. Commun.* **163**, 69–95.
- [31] Vega, J. R., L. M. Gugliotta, and G. R. Meira. (2002). Emulsion copolymerization of acrylonitrile and butadiene: Semibatch strategies for controlling molecular structure on the basis of calorimetric measurements. *Polym. React. Eng.* **10**, 59–82.
- [32] Hsu, S. C., W. Y. Chiu, C. F. Lee, and H. S. Chang. (2001). Composition control of copolymer in semibatch emulsion copolymerization. I: Methyl methacrylate/styrene two-component system. *Polym. J.* **33**, 27–37.
- [33] Aymonier, A., E. Papon, J. J. Villenave, P. Tordjeman, R. Pirri, and P. Gerard. (2001). Design of pressure-sensitive adhesives by free-radical emulsion copolymerization of methyl methacrylate and 2-ethylhexyl acrylate. 1: Kinetic study and tack properties. *Chemi. Mater.* **13**, 2562–2566.
- [34] Gower, M. D. and R. A. Shanks. (2005). Comparison of styrene with methyl methacrylate copolymers on the adhesive performance and peeling master-curves of acrylate pressure sensitive adhesives. *Macromol. Chem. Phys.* **206**, 1015–1027.
- [35] Heatley, F., P. A. Lovell, and T. Yamashita. (2001). Chain transfer to polymer in free-radical solution polymerization of 2-ethylhexyl acrylate studied by NMR spectroscopy. *Macromolecules* **34**, 7636–7641.
- [36] Nielsen, L. E., and R. F. Landel. (1994). *Mechanical Properties of Polymers and Composites*, 2nd ed. New York: Marcel Dekker. p. 141.

Copyright of *International Journal of Polymer Analysis & Characterization* is the property of Taylor & Francis Ltd and its content may not be copied or emailed to multiple sites or posted to a listserv without the copyright holder's express written permission. However, users may print, download, or email articles for individual use.